

Vapor-Induced Swelling of Supported Methacrylic and Siloxane Polymer Films: Determination of Interaction Parameters

Kyriaki Manoli,^{1,2} Dimitris Goustouridis,¹ Ioannis Raptis,¹ Evangelos Valamontes,³ Merope Sanopoulou²

¹*Institute of Microelectronics, NCSR "Demokritos," Ag. Paraskevi Attikis, Athens 15310, Greece*

²*Institute of Physical Chemistry, NCSR "Demokritos," Ag. Paraskevi Attikis, Athens 15310, Greece*

³*Department of Electronics Engineering, TEI of Athens, Athens 12243, Greece*

Received 30 April 2009; accepted 10 July 2009

DOI 10.1002/app.31100

Published online 1 December 2009 in Wiley InterScience (www.interscience.wiley.com).

ABSTRACT: White light reflectance spectroscopy is applied to monitor vapor-induced thickness changes of polymer films, supported on suitable silicon substrates. Assuming unidirectional swelling due to the constraining support, the equilibrium volume swelling of four methacrylic polymers and two siloxane-based copolymers upon exposure to various activities of water, methanol, ethanol, and ethyl acetate vapor, at 30°C is evaluated. The deduced sorption isotherms were fitted to the Flory-Huggins equation and interaction parameters, as well as solubility

coefficients at infinite solute dilution, were deduced for each binary system. The relative sorption capacity of the different classes of polymers toward the four vapors are in line with the expected solubility interactions between solvent and solute. © 2009 Wiley Periodicals, Inc. *J Appl Polym Sci* 116: 184–190, 2010

Key words: white light reflectance spectroscopy; swelling; vapor sorption; thin polymer films; polysiloxanes; polymethacrylates

INTRODUCTION

Sorption of volatile organic compounds (VOCs) and moisture in thin supported polymer films and the ensuing physico-chemical interactions between polymer and analyte are important phenomena in several diverse applications, such as coatings, microelectronics manufacturing, and chemical sensors. The need for proper material selection according to the intended specific application has led to implementation of various methodologies for characterizing vapor-induced changes of supported polymer films, such as quartz crystal microbalance for mass uptake measurements^{1,2} and specular X-ray reflectivity,^{1,3,4} ellipsometry,⁵ or interferometry⁶ for monitoring thickness changes.

Recently, a relatively simple methodology, based on white light reflectance spectroscopy (WLRs), for monitoring thickness (L) changes of supported polymer films induced by sorption of vapors^{7,8} or by temperature variation⁹ has been developed in our lab. In the former case, the information derived from this, or analogous techniques, can be used to estimate the volume fraction of sorbed penetrant,

assuming unidirectional swelling due to the constraining rigid support, or the corresponding mass fraction with the additional assumption of volume additivity upon mixing.^{1,3–7,10} Since experimental time for Fickian diffusion scales with L^2 , the WLRs methodology is considerably faster than gravimetric methods, as usually much thinner films ($L < 1 \mu\text{m}$) are used in the former case. In this respect, it provides a fast and simple means for screening different polymeric materials in respect to their sorptive and swelling behavior in response to various VOC's. In a previous work,⁷ the above methodology was applied to selected polymer-analyte systems (i) to compare the estimated weight gain isotherms with the corresponding literature data obtained by direct gravimetric sorption experiments in bulk free-standing films, and (ii) to study the effect of films thickness, and of substrate, on the fractional swelling of films with thicknesses approaching the radius of gyration of the polymer molecule.

The main objective of this work is to apply the above WLRs methodology for a comparative evaluation of the sorption properties of a series of polymeric materials, in the form of supported films. The polymers tested include three members of a homologous series of relatively hydrophobic poly(alkyl methacrylates), the hydrophilic poly(2-hydroxyethyl methacrylate), and two poly(dimethylsiloxane-*co*-diphenylsiloxane) copolymers, differing in the mole

Correspondence to: M. Sanopoulou (sanopoul@chem.demokritos.gr).

fraction of the constituting co-monomers and in the chemical structure of the terminal groups of the main chain. The thickness expansion of supported films upon exposure to different activities of four vapors of varying polarity and hydrogen-bonding ability were studied. The deduced sorption isotherms were fitted to the Flory-Huggins equation and interaction parameters, as well as solubility coefficients at infinite solute dilution, were deduced for each binary system. The results are discussed in terms of the possible polymer-analyte physico-chemical interactions and the relevant three-dimensional solubility parameters.

THEORETICAL BACKGROUND

Sorption of micromolecular solutes in polymeric materials can be described by the Flory-Huggins theory,¹¹ originally formulated for elastomeric, amorphous polymer-solute systems exhibiting nonpolar or weakly polar interactions. Assuming that the molar volume of solute is much lower than that of polymer, the said theory relates the solute activity in the vapor phase, a_s , to the solute volume fraction in the polymeric phase, ϕ_s , according to eq. (1)

$$\ln a_s = \ln \phi_s + (1 - \phi_s) + \chi(1 - \phi_s)^2 \quad (1)$$

where χ is the Flory-Huggins interaction parameter, assumed constant in the original derivation of the theory, or concentration-dependent in subsequent refinements. Equation (1) with a constant value of χ is commonly used to describe sorption in polymer-vapor systems not necessarily fulfilling the requirements upon which the original theory was derived.

In the simplest case

$$\chi = \frac{\Delta \bar{H}_M}{RT} = \frac{\bar{V}_S(\delta_S - \delta_P)^2}{RT} \quad (2)$$

where $\Delta \bar{H}_M$ (≥ 0) is the partial molar energy of mixing and δ_P , δ_S are the solubility parameters of polymer and solute, respectively, defined as the square root of the cohesive energy densities of the pure components. Equation (2) is a quantitative expression of the general rule "like dissolves like," as it predicts that the maximum solubility of solute in the polymer ($\Delta \bar{H}_M = 0$) is obtained when $\delta_P = \delta_S$.

The concept of solubility parameters has been refined to account for substances exhibiting specific interactions, according to the following expression¹²

$$\delta^2 = \delta_d^2 + \delta_p^2 + \delta_h^2 \quad (3)$$

Where δ_d , δ_p , and δ_h describe dispersion, polar (permanent dipole-permanent dipole) and hydrogen-bonding interactions, respectively. In this case, the

requirement for mutual solubility of polymer and solute is the quantity

$$\begin{aligned} & [(\Delta \delta_d)^2 + (\Delta \delta_p)^2 + (\Delta \delta_h)^2]^{1/2} \\ & = [(\delta_{dP} - \delta_{dS})^2 + (\delta_{pP} - \delta_{pS})^2 + (\delta_{hP} - \delta_{hS})^2]^{1/2} \end{aligned}$$

to be as small as possible.

Because δ_d , δ_p , and δ_h cannot be determined directly, they are usually estimated by group contribution methods.¹² These methods are not expected to provide accurate predictions of the solubility parameters for complex chemical structures. On the other hand, they have been proven very useful for interpreting and correlating the sorption behavior of polymer-solute systems.

EXPERIMENTAL

Materials

Poly(methyl methacrylate) [PMMA] ($M_W \sim 120$ K; d (25°C): 1.188 g/mL, T_g : 96°C), poly(2-hydroxyethyl methacrylate) [PHEMA] ($M_W \sim 300$ K; d (25°C): 1.15 g/mL; T_g : 109°C), poly(*n*-butyl methacrylate) [PBMA] ($M_W \sim 337$ K; d (25°C): 1.07 g/mL; T_g : 15°C), poly(isobutyl methacrylate) [PIBMA] ($M_W \sim 70$ K; d (25°C): 1.09 g/mL; T_g : 55°C) in the form of powder and poly(dimethylsiloxane-*co*-diphenylsiloxane) divinyl terminated [P(DMS-*co*-DPhS)-1] ($M_n \sim 18.9$ K; d (25°C): 1 g/mL; T_g : -90°C; 85 : 15 mole ratio of dimethylsiloxane:diphenylsiloxane), poly(dimethylsiloxane-*co*-diphenylsiloxane) dihydroxy terminated [P(DMS-*co*-DPhS)-2] ($M_n \sim 12$ K; d (25°C): 1.05 g/mL; T_g : -92°C; 95 : 5 mole ratio of dimethylsiloxane : diphenylsiloxane) in liquid form were purchased from Sigma-Aldrich. The T_g values listed above are those given by the supplier, except for PHEMA and the two siloxanes, which were determined by DSC in our lab. Propylene glycol methyl ether acetate (PGMEA), ethyl lactate, ethanol (EtOH), methanol (MeOH), and ethyl acetate (AcOOEt), all of analytical reagent grade, were also purchased from Sigma-Aldrich and used without further purification.

The values of the solubility parameters of all polymers and vapor analytes studied, are listed in Table I. The δ_d , δ_p , and δ_h components were estimated by the group contribution method of Van Krevelen using the values given in Ref. 12, with the exception of the values for the two siloxanes copolymers, which have been calculated by subtraction-addition from values reported in literature for poly(dimethyl siloxane).¹³

Polymer films, supported on oxidized silicon wafers, were prepared by spin-coating from (i) PGMEA solutions of the methacrylic polymers (10% w/w) and of the two polysiloxanes (15% w/w) and (ii) ethyl lactate solutions of PHEMA (6–10% w/w). All supported films were heated on a hot plate for 15 min to 160°C or to 120°C (for those prepared by

TABLE I
Solubility Parameters of Polymers and Solutes Used

	δ_h [(cal/cm ³) ^{1/2}]	δ_p [(cal/cm ³) ^{1/2}]	δ_d [(cal/cm ³) ^{1/2}]	δ [(cal/cm ³) ^{1/2}]
PMMA	9.03	5.70	16.65	19.78
PHEMA	15.82	6.49	16.31	23.63
PBMA	6.96	3.39	17.57	19.20
PiBMA	7.27	3.69	16.59	18.49
P(DMS-co-DPhS)-1	4.87	0.11	22.56	23.20
P(DMS-co-DPhS)-2	4.52	0.10	14.93	15.60
H ₂ O	34.2	31.3	13.3	47.9
MeOH	22.3	12.3	15.2	29.5
EtOH	19.5	8.8	15.8	26.25
AcOOEt	9.2	5.3	15.2	18.6

PGMEA or ethyl lactate solutions, respectively) to remove residual solvent and then were stored in a desiccator until further use. Dry film thicknesses L_0 in the range 200–800 nm were used. The low-thickness limit ensures that the polymer films behave as bulk polymers without any film thickness effects.⁷

Thickness calculation methodology

The principle of WLRS is schematically shown in Figure 1. At each wavelength interference takes place due to the light traveling through the transparent layers, and the final spectrum is recorded to a PC every 2 s. Film thickness changes, due to vapor absorption in the polymer layer, are monitored as changes in the recorded interference spectrum.

In the general case of k -layers, the total incident energy on the spectrometer can be calculated through the effective Fresnel coefficients and several algorithms. In our case, the Abeles approach was followed where the effective Fresnel coefficient is¹⁴

$$\rho_{k-1} e^{i\Delta_{k-1}} = \frac{r_{k-1} + \rho_k e^{i\Delta_k - 2i\delta_{k-1}}}{1 + r_{k-1} \rho_k e^{i\Delta_k - 2i\delta_k}} \quad (4)$$

and r_{k-1} is the Fresnel coefficient. From this set of equations, the reflectance from any k -th layer can be calculated. In the particular case of this study, that is, two transparent layers between the substrate and the environment the total energy can be written in an analytical form⁹:

$$E = \frac{A}{B}$$

$$\begin{aligned} A = & r_{01}^2 + r_{12}^2 + r_{23}^2 + 2r_{01}r_{12}r_{23} + r_{01}^2r_{12}^2r_{23}^2 \\ & + 2r_{01}r_{23} \cos\left(\frac{4\pi}{\lambda}(n_1d_1 + n_2d_2)\right) + 2r_{12}r_{23} \cos\left(\frac{4\pi}{\lambda}n_1d_1\right) \\ & + 2r_{01}r_{12}r_{23}^2 \cos\left(\frac{4\pi}{\lambda}n_2d_2\right) + 2r_{01}r_{12} \cos\left(\frac{4\pi}{\lambda}n_1d_1\right) \\ & + 2r_{01}^2r_{12}r_{23} \cos\left(\frac{4\pi}{\lambda}n_1d_1\right) \end{aligned}$$

$$\begin{aligned} B = & 1 + r_{01}^2r_{12}^2 + r_{01}^2r_{23}^2 + r_{12}^2r_{23}^2 + 2r_{12}r_{23} \cos\left(\frac{4\pi}{\lambda}n_2d_2\right) \\ & + 2r_{01}r_{23} \cos\left(\frac{4\pi}{\lambda}(n_1d_1 + n_2d_2)\right) + 2r_{01}^2r_{12}r_{23} \cos\left(\frac{4\pi}{\lambda}n_2d_2\right) \\ & + 2r_{01}r_{12} \cos\left(\frac{4\pi}{\lambda}n_1d_1\right) + 2r_{01}r_{12}r_{23}^2 \cos\left(\frac{4\pi}{\lambda}n_1d_1\right) \\ & + 2r_{01}r_{12}^2r_{23} \cos\left(\frac{4\pi}{\lambda}(n_1d_1 - n_2d_2)\right) \quad (5) \end{aligned}$$

where n_i is the refractive index of the i -th layer ($i = 0$ for gaseous phase, 1 for the polymeric film, 2 for the SiO₂ layer, and 3 for the Si substrate), d_1 , d_2 the thickness of the polymeric film and of the silicon dioxide, respectively, and λ the corresponding wavelength. The refractive indices n_i of all layers versus wavelength are calculated with a spectroscopic ellipsometer (J.A. Woolam) and fitted to a three parameters (A, B, and C) Cauchy model. Fitting of the experimental spectrum to eq. (5) is performed by using the Levenberg–Marquardt algorithm.¹⁵ Following this methodology, the film thickness is calculated with a precision of ± 0.03 nm.

Absorption experiments are performed in a thermostated chamber ($30 \pm 0.5^\circ\text{C}$). The desired penetrant activity $a_S (= p/p_{\text{sat}}$, where p_{sat} is the saturation

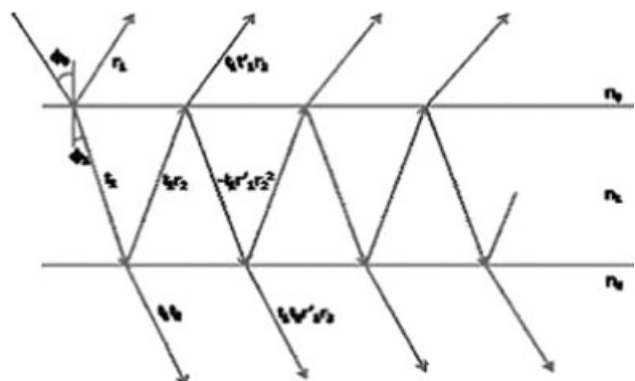


Figure 1 Schematic representation of interference taking place at the interfaces of the various layers (see text).

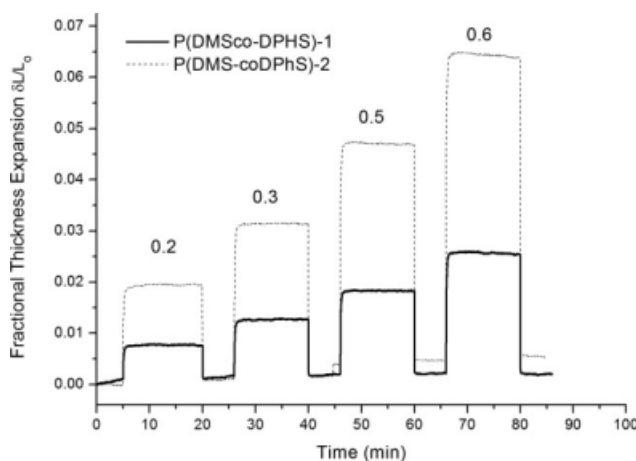


Figure 2 Typical thickness expansion-contraction curves obtained when initially dry, supported P(DMS-*co*-DPhS)-1 and P(DMS-*co*-DPhS)-2 films are subjected to successive equilibration with progressively higher vapor ethanol activities a_S (indicated by the numbers on the plot) with intervening desorption steps back to $a_S = 0$.

pressure of the vapor at 30°C) is generated by mixing nitrogen with saturated penetrant vapor at 30°C and atmospheric pressure, and the mixture passes at a rate of 1000 mL/min (controlled by mass flow controllers) through the chamber containing the supported film, with its upper surface exposed to the stream.^{7,8}

In what follows, the dry polymeric film thickness (d_1) in eq. (5), is denoted as L_0 and any film thickness changes as δL . Each dry film was subjected to series of absorption runs involving successive equilibration with progressively higher vapor activities a_S with intervening desorption steps back to $a_S = 0$, effected by passing pure N_2 though the chamber. A typical example is shown in Figure 2. From the equilibrium expansion data, the fractional film expansion $\delta L/L_0$ at each activity was determined. Assuming one-directional swelling of the supported film along the thickness direction, that is, $\delta L/L_0 = \delta V/V_0$, the volume (ϕ_S) fraction of penetrant in the polymer-penetrant mixture is given by

$$\phi_S = \delta L / (L_0 + \delta L_0) \quad (6)$$

In fitting the experimental spectra to eq. (5), the refractive index of the polymer, n_1 , is assumed constant during absorption of the vapor penetrant. The error induced by this assumption is expected to be significant at high degrees of swelling and/or large differences between η_1 and the refractive index of solute, η_S , and can be roughly estimated from the calculated ϕ_S values [eq. (6)], on the basis of the Clausius–Mossotti mixing rule

$$\frac{\eta_{PS}^2 - 1}{\eta_{PS}^2 + 2} = \frac{\eta_1^2 - 1}{\eta_1^2 + 2} (1 - \phi_S) + \frac{\eta_S^2 - 1}{\eta_S^2 + 2} \phi_S \quad (7)$$

For the highest ϕ_S values determined during sorption experiments (i.e., $\phi_S \sim 0.1$ and ~ 0.17 for sorption of H_2O in PHEMA and for sorption of AcOOEt in P(DMS-*co*-DPhS)-2, respectively), the said error was estimated to be $\sim 1.3\%$, whereas in most other cases it was $< 1\%$.

RESULTS AND DISCUSSION

Sorption isotherms

The ϕ_S versus a_S data for all systems studied are shown in Figures 3–6. In each of these figures the sorption data of all polymers for the same vapor analyte are presented. [For reasons of clarity, the methanol data have been split in two plots, Fig. 4(a,b)]. For each system, the results obtained from films of different thicknesses are in satisfactory agreement. Each sorption isotherm was fitted, by nonlinear regression analysis, to eq. (1), and the derived values of χ are listed in Table II. Fitting (shown also in the same figures) is fairly satisfactory for most systems. Sorption in glassy polymers at low activities [e.g., sorption of MeOH in PHEMA and PMMA, see Fig. 4(b)] is characterized by an initially convex-upward isotherm, which is probably associated with adsorption in pre-existing cavities that constitute the excess free volume of a glassy polymer matrix, and cannot be accounted for, by the Flory-Huggins theory.

Among the polymers studied, PHEMA, due to the pendant OH group promoting hydrogen-bonding

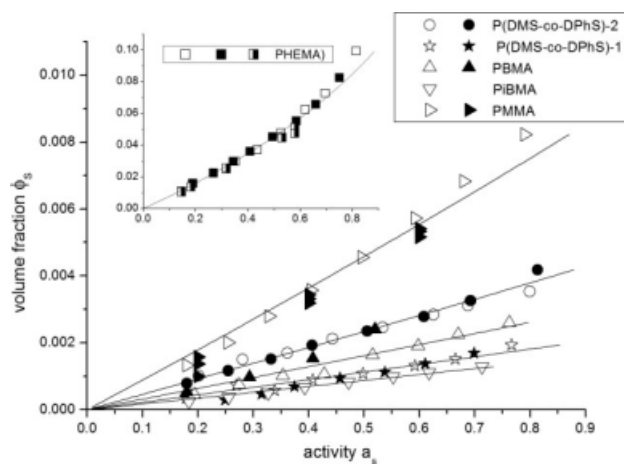


Figure 3 Sorption isotherm of H_2O vapor in polymer films, supported on Si/SiO₂ substrate, at 30°C (points) and fitting to eq. (1) (lines). L_0 (nm): (□) 606 nm, (■) 517 nm, (◐) 273 nm, (○) 240 nm, (●) 244 nm, (☆) 197 nm, (★) 205 nm, (△) 515 nm, (▲) 530 nm, (▽) 600 nm, (▷) 737 nm, and (◑) 370 nm.

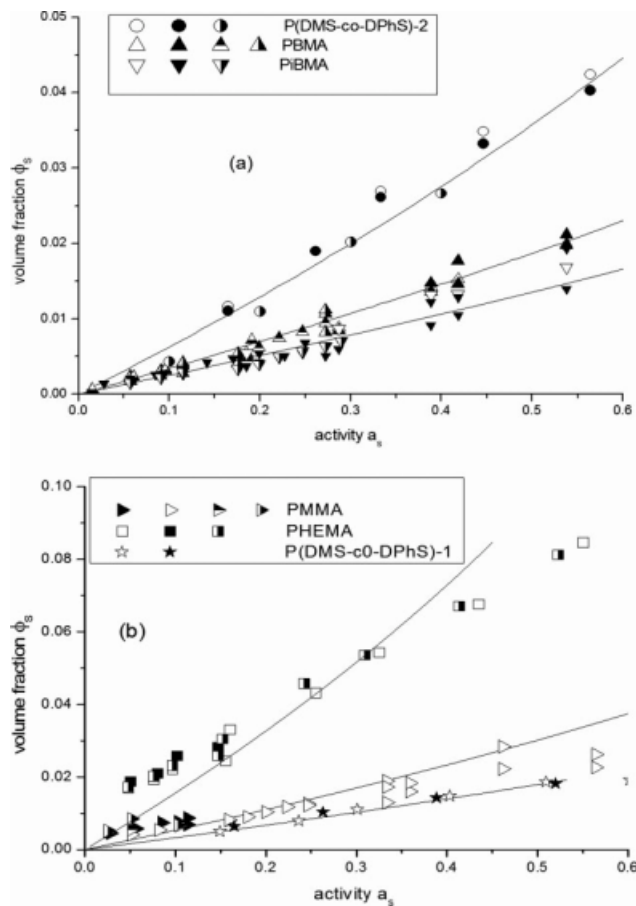


Figure 4 Sorption isotherm of MeOH vapor in polymer films, supported on Si/SiO₂ substrate, at 30°C (points) and fitting to eq. (1) (lines). (a) L_0 (nm): (Δ) 515 nm, (\blacktriangle) 530 nm, (\triangle) 486 nm, (Δ) 520 nm, (\circ) 244 nm, (\bullet) 719 nm, (∇) 600 nm, (\blacktriangledown) 580 nm, (\triangledown) 570 nm, (b) L_0 (\star) 197 nm, (\blackstar) 205 nm, (\triangleright) 172 nm, (\blacktriangleright) 220 nm, (\blacktriangleleft) 320 nm, (\blacktriangleright) 560 nm, (\square) 606 nm; (\blacksquare) 517 nm, and (\square) 300 nm.

ability and polarity (Table I), exhibits the highest sorptive capacity for H₂O, MeOH, and EtOH, and the lowest for AcOOEt (Figs. 3–6). At the low solubility end for H₂O (Fig. 3) and MeOH (Fig. 4) stands PiBMA, closely followed by P(DMS-*co*-DPhS)-1. The latter polymer exhibits only slightly higher sorptive capacity toward H₂O and MeOH, as compared with PiBMA, and the lowest affinity toward EtOH among all polymers studied (Fig. 5).

Among the relatively hydrophobic methacrylic polymers PMMA, PBMA, and PiBMA, the results of Figure 3 indicate that PMMA is the more susceptible to sorption of H₂O. The differences in the sorptive capacity among these polymers progressively fade out as we move to sorption of MeOH (Fig. 4) and finally EtOH (Fig. 5). Thus, PiBMA, exhibiting the lowest affinity for H₂O, is the most suitable for discriminating alcohols from H₂O.

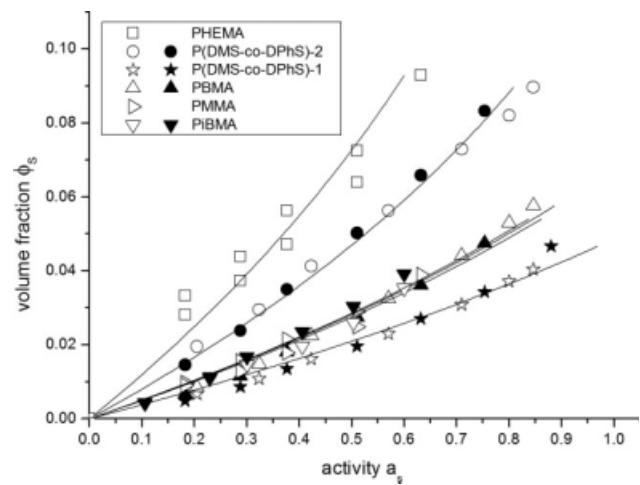


Figure 5 Sorption isotherm of EtOH vapor in polymer films, supported on Si/SiO₂ substrate, at 30°C (points) and fitting to eq. (1) (lines). L_0 (nm): (\square) 606 nm, (\circ) 240 nm, (\bullet) 170 nm, (\star) 197 nm, (\blackstar) 205 nm, (\triangle) 530 nm, (\triangleright) 270 nm, (∇) 567 nm, and (\blacktriangledown) 855 nm.

Comparison of the two siloxane-based copolymers, shows that of P(DMS-*co*-DPhS)-2 has a higher affinity toward all vapors studied, as compared with P(DMS-*co*-DPhS)-1, possibly due to the presence of the terminal OH groups in the former polymer. Abraham,¹⁶ using two commercial poly(methylphenylsiloxane)s as the stationary phase in gas-liquid chromatography, found that the presence of OH groups in the structure of both polymers (evidenced in their IR spectra) measurably influences their sorption properties. The effect of OH groups was reflected in the estimated hydrogen-bonding acidity and dipolarity/polarizability constants of the

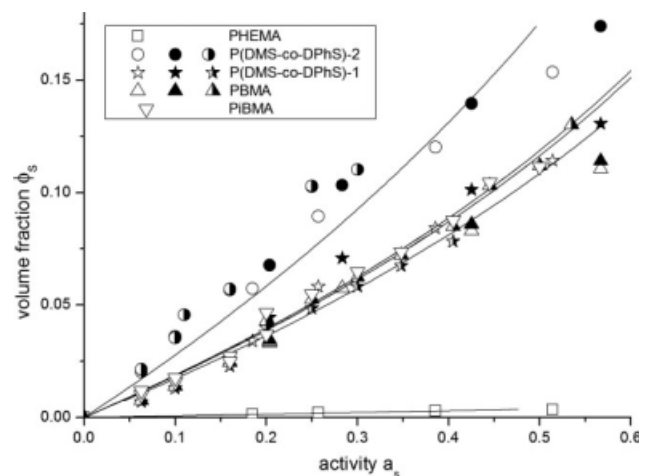


Figure 6 Sorption isotherm of AcOOEt vapor in polymer films, supported on Si/SiO₂ substrate, at 30°C (points) and fitting to eq. (1) (lines). L_0 (nm): (\square) 755 nm, (\circ) 380 nm, (\bullet) 395 nm, (\circ) 1395 nm, (\star) 197 nm, (\blackstar) 205 nm, (\star) 1450 nm, (\triangle) 530 nm, (\blacktriangle) 515 nm, (\triangle) 850 nm, and (∇) 558 nm.

TABLE II
Flory-Huggins Interaction Parameters Derived from Fitting the Data of Figures 3–6 to eq. (1)

	H ₂ O	MeOH	EtOH	AcOOEt
PHEMA	1.58 (0.01)	0.90 (0.05)	1.16 (0.06)	3.95 (0.05)
PMMA	3.73 (0.02)	1.95 (0.05)	2.04 (0.03)	
PBMA	4.75 (0.03)	2.39 (0.01)	2.01 (0.01)	0.96 (0.04)
PIBMA	5.36 (0.02)	2.69 (0.03)	2.02 (0.02)	0.72 (0.02)
P(DMS- <i>co</i> -DPhS)-1	5.11 (0.03)	2.43 (0.02)	2.28 (0.02)	0.73 (0.03)
P(DMS- <i>co</i> -DPhS)-2	4.39 (0.01)	1.81 (0.02)	1.55 (0.02)	0.21 (0.04)

The standard error is given in parentheses.

polymers. These constants are included in linear solvation energy relationships equations¹⁷ that provide a more elaborate treatment of solute–solvent interactions than that of three-dimensional solubility parameters.

Quantification of the extent of sorption, by the values of χ presented in Table II, allows some additional comments, as well as comparison with literature values derived from direct gravimetric measurements in free-standing films. In general, in cases of interactions other than those due to dispersion forces, solubility is favored for polymer–solute systems, of similar polarity and hydrogen-bonding ability. Thus, in the case of PHEMA, the lower values of χ (and higher sorptive capacity) characterizing sorption of MeOH and EtOH as compared with sorption of H₂O (Table II) can be attributed to the corresponding lower δ_H , δ_P values of the alcohols, being closer to those of PHEMA. Similar arguments can be invoked for the higher sorptive capacity of each of the remaining methacrylic polymers toward alcohols as compared with water.

On a quantitative basis, the χ value for the system PHEMA–H₂O ($\chi = 1.6$) is close to the corresponding values of 1.4–1.5 derived by Rodriguez et al.¹⁸ from gravimetric measurements on free-standing films. On the other hand, in PMMA, the χ values for H₂O ($\chi = 3.7$) and MeOH ($\chi = 1.8$) are higher (and sorption levels lower) than the corresponding literature values ($\chi = 3$ –3.3 for H₂O in Ref. 18 and 1.1–1.28 for MeOH in Ref. 19). A possible reason for the lower sorption levels estimated here is the fact that supported films may not attain full volume swelling equilibrium due to the constraints imposed on lateral swelling by the support.^{6,7} This effect is expected to be important at low degrees of swelling in rigid polymers (as is the case of the PMMA–H₂O and PMMA–MeOH systems) and will result in actual reduced ϕ_S values as compared with the free-standing films used in Refs. 18 and 19. As to the siloxane copolymers, due to the lack of relevant literature data, results can only be compared with data on crosslinked PDMS. Thus for PDMS, values of χ

range from 4.45 ± 2.16^{20} to 5.3^{21} for sorption of H₂O, from 2.5^{22} to 3.14 ± 0.40^{20} or 3.21^{21} for sorption of MeOH and from 2.19^{23} to 2.46^{24} for sorption of EtOH. These values (i) better compare with those of Table II for P(DMS-*co*-DPhS)-1, than for the OH-terminated P(DMS-*co*-DPhS)-2 and (ii) indicate that PDMS has an increasing sorptive capacity as we move from H₂O to MeOH and finally EtOH, as is the case for the two siloxane-based polymers studied here.

Solubility coefficients

An estimate of the solubility, or partition, coefficient S at the limit of infinite dilution, expressed as the ratio of the solute volume fraction in the polymeric phase over the solute activity in the external vapor phase ($S = \phi_S/a_S$), can be obtained on the basis of eq. (1). For $\phi_S \ll 1$, eq. (1) reduces to

$$\phi_S/a_S = \exp(-1 - \chi) \quad (8)$$

where $\exp(-1 - \chi)$ is the limiting inverse Henry's law constant of the system.¹¹

The values of S calculated on the basis of eq. (8) have been correlated to the differences of the solubility parameters between solute and polymer (Table I) of each binary system. The correlation, shown in Figure 7 indicates a sharp decay of solubility coefficient with increasing $\Delta\delta$. Thus, with the exception of the data points referring to the PHEMA–H₂O and PHEMA–AcOOEt systems, we observe that polymer–solute pairs characterized by solubility coefficients, S , in the range of 0.1–0.3 are grouped at the low $\Delta\delta$ end of the plot ($\Delta\delta \leq 10 \text{ cal}^{1/2}/\text{cm}^{3/2}$), whereas systems with S values lower by more than one order of magnitude ($S \leq 0.008$) are concentrated at the high

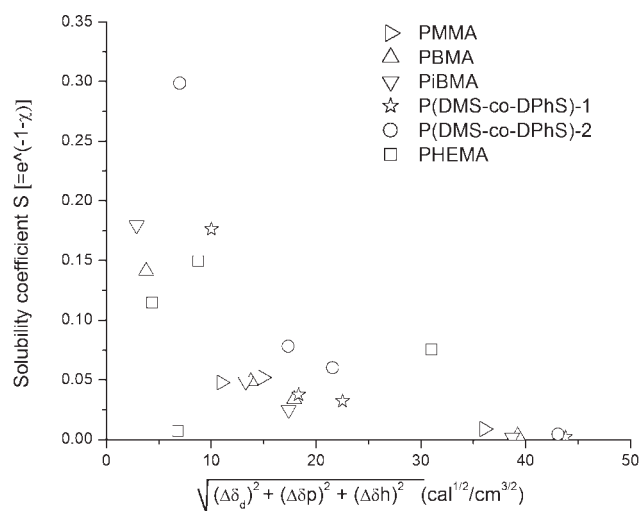


Figure 7 Correlation of solubility coefficients S with three-dimensional solubility parameter differences.

$\Delta\delta$ end of the plot ($\Delta\delta > 35 \text{ cal}^{1/2}/\text{cm}^{3/2}$). Finally, systems exhibiting intermediate values of S ($0.02 \leq S \leq 0.08$) are located at values of $\Delta\delta$ ranging from 10 to $25 \text{ cal}^{1/2}/\text{cm}^{3/2}$. The correlation of Figure 7 confirms the usefulness of the concept of solubility parameters for a rough screening of polymeric materials on the basis of their swelling capacity towards different analytes.

CONCLUSIONS

The sorptive capacity of various polymers toward four vapor analytes has been studied by application of an interferometric methodology for measuring vapor-induced thickness changes of supported polymeric films. In general, the deduced sorption isotherms could be adequately described, by the Flory-Huggins equation, and the relative sorption capacity of the different classes of polymers toward the four vapors are in line with the expected solubility interactions between solvent and solute. The results indicate that the applied optical methodology is suitable for screening polymeric materials for specific applications, such as chemical sensors, on the basis of their sorption properties.

References

- Vogt, B. D.; Soles, C. L.; Lee, H.-J.; Lin, E. K.; Wu, W. *Langmuir* 2004, 20, 1453.
- Dubreuil, A. C.; Doumenc, F.; Guerrier, B.; Allain, C. *Macromolecules* 2003, 36, 5157.
- Vogt, B. D.; Prabhu, V. M.; Soles, C. L.; Satija, S. K.; Lin, E. K.; Wu, W. *Langmuir* 2005, 21, 2460.
- Beck Tan, N. C.; Wu, W. L.; Wallace, W. E.; Davis, G. T. *J Polym Sci Part B: Polym Phys* 1998, 36, 155.
- Wind, J. D.; Sirard, S. M.; Paul, D. R.; Green, P. F.; Johnston, K. P.; Koros, W. J. *Macromolecules* 2003, 36, 6433.
- Stamatialis, D. F.; Wessling, M.; Sanopoulou, M.; Strathmann, H.; Petropoulos, J. H. *J Membr Sci* 1997, 130, 75.
- Manoli, K.; Goustouridis, D.; Chatzandroulis, S.; Raptis, I.; Valamontes, E. S.; Sanopoulou, M. *Polymer* 2006, 47, 6117.
- Goustouridis, D.; Manoli, K.; Chatzandroulis, S.; Sanopoulou, M.; Raptis, I. *Sens Actuators B* 2005, 111, 549.
- Vourdas, N.; Karadimos, G.; Goustouridis, D.; Gogolides, E.; Boudouvis, A. G.; Tortai, J.-H.; Beltsios, K.; Raptis, I. *J Appl Polym Sci* 2006, 102, 4764.
- Jaczewska, J.; Raptis, I.; Budkowski, A.; Goustouridis, D.; Raczowska, J.; Sanopoulou, M.; Pamuła, E.; Bernasik, A.; Rysz, J. *Synth Met* 2007, 157, 726.
- Flory, P. J. *Principles of Polymer Chemistry*; Cornell University Press: London, 1953.
- Van Krevelen, D. W. *Properties of Polymers*, 3rd ed.; Elsevier Science Publishers: Amsterdam, 1990.
- Uragami, T.; Yamada, H.; Miyata, T. *J Membr Sci* 2001, 187, 255.
- Heavens, O. S. *Optical Properties of Thin Solid Films*; Dover Publications Inc.: Mineola, New York, 1991.
- Marquardt, D. *J Soc Ind Appl Math* 1963, 11, 431.
- Abraham, J. *J Chromatogr* 1991, 588, 361.
- Grate, J. W.; Abraham, M. H. *Sens Actuators B* 1991, 3, 85.
- Rodriguez, O.; Fornasiero, F.; Arce, A.; Radke, C. J.; Prausnitz, J. M. *Polymer* 2003, 44, 6323.
- Dimos, V.; Sanopoulou, M. *J Appl Polym Sci* 2005, 97, 1184.
- Lue, S. J.; Wu, S. Y.; Wang, S. F.; Wang, L. D.; Tsai, C. L. *Desalination* 2008, 233, 286.
- Favre, E.; Schaetzel, P.; Nguyen, Q. T.; Clement, R.; Neel, J. *J Membr Sci* 1994, 92, 169.
- Mandal, S.; Pangarkar, V. G. *J Membr Sci* 2002, 201, 175.
- Ghoreyshi, S. A. A.; Farhdpour, F. A.; Soltanich, M. *Desalination* 2002, 144, 93.
- Chandak, M. V.; Lin, Y. S.; Ji, W.; Higgins, R. J. *J Appl Polym Sci* 1998, 67, 165.